The NQR and NMR studies of icosahedral borides

1999 J. Phys.: Condens. Matter 11 4435

(http://iopscience.iop.org/0953-8984/11/22/314)

J. Phys.: Condens. Matter **11** (1999) 4435–4450. Printed in the UK PII: S0953-8984(99)97678-6

The NQR and NMR studies of icosahedral borides

Donghoon Lee†§, Philip J Bray†‖ and Terry L Aselage‡¶

† Department of Physics, Box 1843, Brown University, Providence, RI 02912, USA
‡ Advanced Materials and Device Sciences, Department 1153, MS 1421,
Sandia National Laboratories, Albuquerque, NM 87185, USA

Received 18 September 1998, in final form 24 March 1999

Abstract. Boron NMR and NQR studies have been performed on three icosahedral borides: α- and β-rhombohedral boron and boron carbide ($B_{12}C_3$). Two ^{11}B NMR peaks, separated by significant chemical shifts in the range from 130 ppm to 280 ppm, were clearly observed for all of the icosahedral borides that were not enriched in the ^{10}B isotope. A single peak, however, was found for the ^{10}B enriched boron carbide powder (90.6 at.% enrichment.) Moreover, the peak separation in the ^{11}B NMR spectrum for the unenriched β-boron was reduced when the sample was crushed into a fine powder. In addition to NMR responses, four strong NQR responses were observed for boron carbides from different manufacturers. Two resonance signals, observed at 513 kHz and 2769 kHz, correspond to one of the icosahedral boron sites and the boron in the CBC chain, respectively. The other two NQR responses, having frequencies of 361 and 380 kHz, are either ^{10}B responses for the chain site or ^{11}B responses for the other boron sites in the icosahedra. The NQR responses are not only consistent with the previous NMR studies performed independently by Silver and Bray (1959 *J. Chem. Phys.* **31** 247) and by Hynes and Alexander (1971 *J. Chem. Phys.* **54** 5296, 1972 *J. Chem. Phys.* Erratum **56**), but also provide much higher accuracy for the values of the quadrupolar parameters.

1. Introduction

Boron carbides are very important materials for structural applications because of their hardness, wear resistance, reasonably low density and very low thermal conductivities. Also, because of their very high melting temperatures (up to 2400 °C), and their electronic transport properties, the boron carbides are exceptionally good very-high-temperature p-type thermoelectric materials [1]. Despite their extensive use, the structures of these materials have not been determined with certainty. Since Silver and Bray [2] determined by NMR the existence in $B_{12}C_3$ of a boron atom at the centre of what had been thought to be a three-carbon chain (–C–C–C–) in the rhombohedral unit cell, several investigations have supported that result. In the present study, both NMR and NQR (nuclear quadrupole resonance) methods are used for structural studies of $B_{12}C_3$ and other icosahedral boron-rich solids such as α-rhombohedral boron and β-rhombohedral boron (i.e., β-boron). Strong NQR responses were obtained from boron atoms in the C–B–C chains in $B_{12}C_3$, along with several other NQR responses from boron atoms in the icosahedra. These NQR results are consistent with the NMR studies by Silver and Bray [2], and those by Hynes and Alexander [3]. In addition, ^{11}B NMR in two

§ Present address: Department of Physics, Pai Chai University, Taejon, Korea.

‖ Research at Brown University supported by the National Science Foundation through grant DMR 89-20532.
¶ Work at Sandia National Laboratories was supported by the Office of Basic Energy Sciences, USDOE under contract No DE-AC04-94AL85000. Sandia is a multiprogram laboratory operated by the Lockheed Martin Co. for the USDOE.

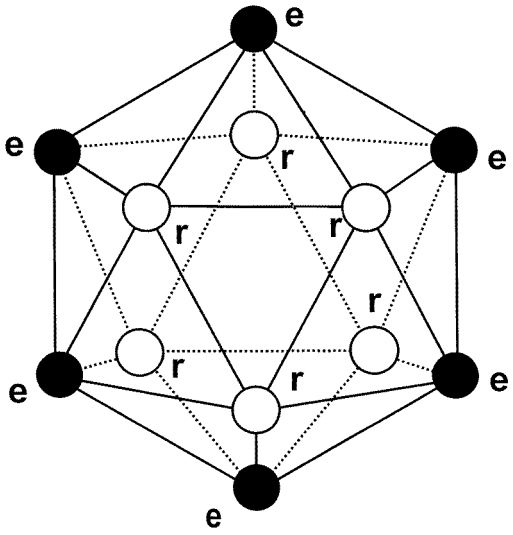

Figure 1. Structure of an icosahedron: six atoms in the equatorial sites, specified by 'e', form a staggered belt around an equator of the icosahedron and the other six atoms are in the rhombohedral sites.

different fields, 1.17 and 7.05 Tesla, revealed the possibility of chemical shifts due to two distinct boron sites in the icosahedra. The two different fields were also used in order to obtain structural information from ^{11}B NMR spectra for α-rhombohedral boron and β-boron.

2. The structure of boron

Three forms of crystalline boron are known to exist: α-rhombohedral boron (B_{12}), α-tetragonal boron (B_{50}) and β-boron (B_{105}). (The subscript number to the right of an atomic symbol indicates the number of atoms in a unit cell.) Since an icosahedron is the basis of the α-rhombohedral boron (B_{12}) structure, the α-tetragonal boron (B_{50}) structure, β-boron (B_{105}) and boron carbides ($B_{(1-x)}C_x$, $0.1 \leqslant x \leqslant 0.2$), the icosahedral structure will be reviewed here. The icosahedra in these borides have two types of site, labelled 'r' and 'e' in figure 1. The rhombohedral site is denoted by 'r', and 'e' indicates an equatorial site. The rhombohedral site is coordinated to another icosahedron, while the equatorial site either contributes to a three-centre bond (in α-rhombohedral boron (B_{12})) or is coordinated to a terminal atom in the chain site along the body diagonal of a rhombohedron (in some boron pnictides and boron carbides). Fivefold axes of symmetry pass through all of the vertices of an ideal icosahedron, but that symmetry is only approximate for the actual materials discussed here.

3. The structure [4] of α-rhombohedral boron (B_{12})

α-rhombohedral boron (B_{12}) has 12 boron atoms in a unit cell: half of the boron atoms (those in the rhombohedral sites) are bonded to other icosahedra (six-coordinated borons), and the other six boron atoms (those in the equatorial sites) form three-centre bonds. Eight icosahedra form a rhombohedron as shown in figure 2. The structure of α-rhombohedral boron (B_{12}) is very important since it contains the basic icosahedral framework of boron-rich solids such as β-boron, boron pnictides and boron carbides.

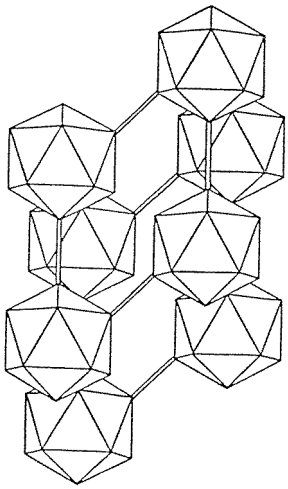

Figure 2. Structure of α-rhombohedral boron: eight icosahedra, which have boron atoms on all of their vertices, form a rhombohedron.

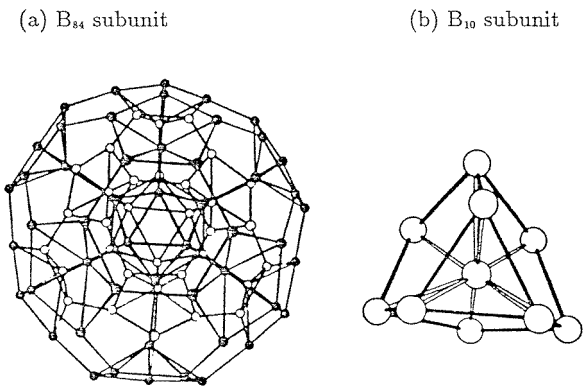

Figure 3. The structures of two subunits for β-rhombohedral boron [B_{105} or $B_{84}(B_{10}B\,B_{10})$]. The two subunits are the B_{84} subunit (a) and the B_{10} subunit (b).

4. The structure of β-boron

The structure [5] of β-boron B_{105} can be visualized as (B_{84}) ($B_{10}BB_{10}$). The B_{84} subunit (figure 3(a)) consists of an icosahedron bonded to 12 half-icosahedra at the 12 vertices of the icosahedron. In the rhombohedral cell, one B_{84} subunit is located at each vertex of the rhombohedron. Within the rhombohedral cell along the diagonal axis are ($B_{10}BB_{10}$) groups. Figure 3(b) displays the B_{10} subunit. Five different boron sites are expected for β-boron. Two sites are expected within the B_{84} subunit: one, a six-coordinated site (site 1 in table 1), in the rhombohedral position in the icosahedron, and the other (site 2), possibly a six-coordinated site, in the equatorial position. In the B_{10} subunit there are three sites: the nine atoms on the pentagonal faces are eight-coordinated (site 3); the centre boron atom is nine-coordinated (site 4) and along the diagonal axis within the rhombohedral unit one boron atom which has an octagonal symmetry is located in between two B_{10} subunits (site 5). The site information is summarized in table 1.

Table 1. The boron site information for β-rhombohedral boron.

Site	Number of boron atoms	Coordination	Boron atom proportion (%) in unit cell
1	48	6	45.7
2	36	6[a]	34.3
3	18	8	17.1
4	2	9	1.9
5	1	[a]	1.0

[a] Uncertain.

5. Structure of the boron carbides

Structures of the boron carbides have been in controversy for about a half century [6, 7]. The boron carbides ($B_{1-x}C_x$) exist as a single-phase material over a significant range of carbon concentration, $0.1 \leqslant x \leqslant 0.2$ [8–10]. The present study is restricted to the case of $x = 0.2$, i.e., $B_{12}C_3$ or B_4C. (The single-phase region of boron carbides extends only to about 19–19.5 at.% carbon, but the conventional formula $B_{12}C_3$ with $x = 0.20$ will be retained in this paper.) X-ray studies by Zhdanov and Sevast'yanov [6] and by Clark and Hoard [11] have determined the boron carbide structure and have obtained two distinct boron positions, denoted $6h_1$ and $6h_2$. According to the latter workers, the structural units of boron carbide are composed of a linear chain of three carbon atoms and a group of 12 boron atoms located at the vertices of an icosahedron. A boron atom in the $6h_1$ position is bonded to five neighbouring boron atoms in the icosahedron and to one carbon in the chain position, termed the 2c position. A boron atom in the $6h_2$ position is bonded to five neighbouring boron atoms in the icosahedron and to another boron atom in an adjacent icosahedron. Hence, the two icosahedral sites for boron carbides, $6h_1$ and $6h_2$, are located at the equatorial and rhombohedral positions, respectively (see figure 1). An earlier NMR study [2] showed that a boron atom is in the centre of the three-atom chain; that is, the chain is a (CBC) chain rather than a (CCC) chain. This boron site is termed the 1b site. The substitution of a boron atom for a carbon atom in the centre of the CBC chain suggests that a carbon atom is present within the icosahedra of $B_{12}C_3$: ($B_{11}C$)(CBC). Analyses [7, 12, 13] of spectroscopic, structural and electronic transport data as well as considerations of the free energies of boron carbides [14] show that the icosahedra of boron carbides preferentially retain a carbon atom even as the carbon content is reduced from $B_{12}C_3$.

When one accepts the existence of the (CBC) chain rather than the (CCC) chain, the structure of the icosahedron in $B_{12}C_3$ becomes complex since a carbon atom goes into an icosahedron to make ($B_{11}C$)(CBC) (see figure 4). In terms of boron sites, there will be two possibilities: the carbon atom can exist in either the $6h_1$ or the $6h_2$ site. In either case, five boron sites could be expected: one from the CBC chain and the others from each icosahedron. However, evidence from Raman spectra [13, 14] and x-ray diffraction refinements [15] suggests that carbon and other heteroatoms in boron icosahedra preferentially reside within the rhombohedral sites, $6h_2$.

Having a carbon atom in the icosahedron in a $6h_2$ site, boron atoms in the rhombohedron experience many local environments. One site is the 1b site in the centre of the CBC chain. The rest of the boron sites are located in the icosahedron and differ in both their crystal site and in their neighbouring atoms. One site is the $3h_1$ site which links five boron atoms in the icosahedron and the carbon atom at the CBC chain site; one site is the $3h_1^*$ site which links four boron atoms in the icosahedron, a carbon atom in the CBC chain and the carbon atom in the icosahedron; one site is the $3h_2$ site which links 5 boron atoms in the icosahedron and either a boron atom in an adjacent icosahedron or a carbon atom in an adjacent icosahedron;

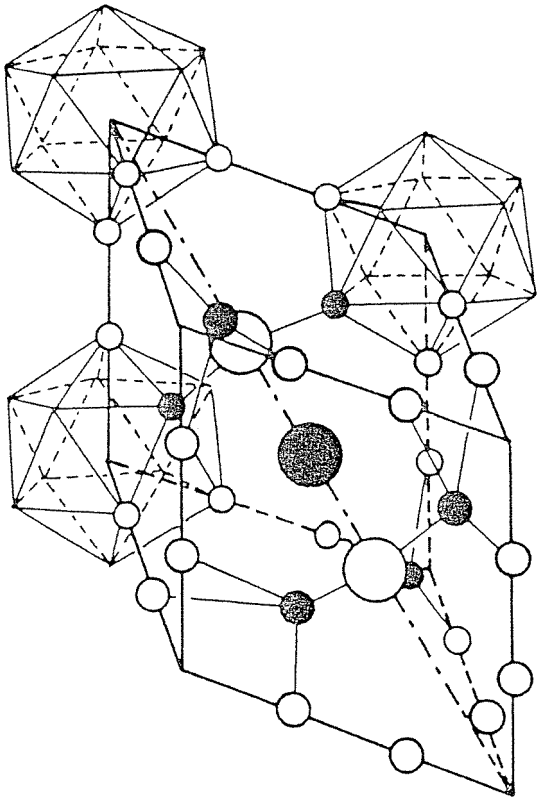

Figure 4. The structure of boron carbide [$B_{12}C_3$ or B_{11}(CBC)]. The small white circles are borons in the $6h_2$ sites (or the equatorial sites); two large white circles are carbon atoms in the CBC chain and the large black circle in between the two large white circles is a boron atom in the 1b site.

Table 2. Boron site information for $B_{12}C_3$ in the case of a carbon atom in the $6h_2$ site. All of the numbers from the second column of the sixth column describe the numbers of participating atoms. Definition of the symbols in the table: B means the number of boron atoms in the particular type of site (e.g., the 1b site); 1-B means the number of boron atoms (either in the same or another icosahedron) linked to a boron in the designated site; 1-C means the number of carbon atoms (in a CBC chain or in the same or another icosahedron) linked to a boron in the designated site.

Site	B	1-B in the icosahedron	1-B in another icosahedron	1-C in the CBC chain	1-C in the icosahedron	1-C in another icosahedron
1b	1	0	0	2	0	0
$3h_1$	3	5	0	1	0	0
$3h_1^*$	3	4	0	1	1	0
$3h_2$	3	5	1[a]	0	0	1[a]
$2h_2^*$	2	4	1[a]	0	1	1[a]

[a] The designated site links either a boron in an adjacent icosahedron or a carbon atom in an adjacent icsoahedron.

one site is the $2h_2^*$ site which links four boron atoms in the icosahedron, the carbon atom in the icosahedron and either a boron atom in an adjacent icosahedron or a carbon atom in an adjacent icosahedron. This site information is tabulated in table 2.

Each of the various boron bonding configurations noted above can produce its own unique set of electron distributions at the various boron sites. Since the electron distribution determines the chemical shift of the NMR response from the boron at a particular site, the total NMR spectrum of the material may consist of a complex of individual responses (if the differences in chemical shifts between sites are sufficient to permit resolution of the responses from each other).

6. Previous NMR studies of $B_{12}C_3$

Silver and Bray studied a single crystal of boron carbide ($B_{12}C_3$) by NMR [2]. The strong observed resonance varied in frequency as the crystal was placed in various orientations in the magnetic field, a situation arising from the interaction of the ^{11}B nuclear electrical quadrupole moment with the gradient of the electric field at the nuclear site. Analysis of the spectrum as a function of crystal orientation showed that the nuclear site is on the axis of the previously labelled 'C–C–C chain', and that most or all of the chain sites in the rhombohedra are CBC rather than CCC. The values of the quadrupole coupling constant Q_{cc} and the asymmetry parameter η for boron atoms in the centres of the CBC chains, or the 1b position, are 5.58 ± 0.02 MHz and 0, respectively, at room temperature. (The quadrupole coupling constant $Q_{cc} = e^2 q Q/h$ where Q is the nuclear electrical quadrupole moment and $q = V_{zz}$. V is the electrical potential at the nuclear site from charges outside the nucleus, and V_{xx}, V_{yy} and V_{zz} where $V_{xx} = \partial^2 V/\partial x^2$ are the components of the electric field gradient (EFG) tensor at the nuclear site in the principal axis system of the tensor. The asymmetry parameter $\eta = (V_{xx} - V_{yy})/V_{zz}$ is a measure of the departure of the EFG from cylindrical symmetry, and $0 \leqslant \eta \leqslant 1$.) Hynes and Alexander [3] confirmed that the chain inside a rhombohedron is a CBC chain rather than a CCC chain. Their Q_{cc} value of the 1b site was 5.48 MHz at room temperature.

7. NQR studies

In the absence of an applied magnetic field, the quadrupole interaction (whose strength is given by Q_{cc}) will set up a system of energy levels, and transitions between those levels can be stimulated and monitored as in standard NMR experiments. This 'zero-field NMR' or 'nuclear electrical quadrupole resonance' (NQR) can be carried out for boron. For a nuclear spin $I = \frac{3}{2}$ (the case for the ^{11}B isotope) an NQR transition frequency ν_Q is calculated from the following equation [16]:

$$\nu_Q = \frac{Q_{cc}}{2}\sqrt{1 + \frac{\eta^2}{3}}. \tag{1}$$

Then the NQR transition frequency of the 1b site is expected to be 2.79 ± 0.01 MHz at room temperature. NQR studies of $B_{12}C_3$ are reported later in this paper.

8. Sample preparation

α-rhombohedral boron was supplied as a reddish chunk by Dr G P Tsiskarishvili of the Institute for Metallurgy in Tbilisi, Georgia. β-boron and ^{10}B enriched $B_{12}C_3$ was prepared by one of the authors (TLA). $B_{12}C_3$ powder enriched to 90.6 at.% in the ^{10}B isotope was obtained from Eagle–Picher Industries. The powder was annealed at 1850 °C for 4 h in a vacuum of 1×10^{-4} Torr, then cooled to room temperature in gettered argon. The hexagonal unit

cell parameters determined by x-ray powder diffraction, $a = 5.603$ Å and $c = 12.078$ Å, and the Raman spectra of the sample were consistent with the annealed sample having a carbon concentration near $B_{12}C_3$. A $B_{12}C_3$ powder sample having the natural isotopic abundance of boron was prepared in our laboratory from high-purity starting materials using procedures described elsewhere [17]. (This material will be referred to as the 'high-purity $B_{12}C_3$ powder' throughout this paper.) Five commercial $B_{12}C_3$ powders were obtained from different manufacturers: Alfa, Atomergic, Fluka, ICN and Pfaltz and Bauer. α-tetragonal boron was not available for the studies reported here. A portion of the β-boron sample was crushed into a fine powder.

9. Experiment

The ^{11}B NMR static spectra were obtained for α-rhombohedral and β-boron and all boron carbide samples (^{10}B enriched and unenriched and five commercial $B_{12}C_3$ powder samples) by CW (continuous wave) NMR, operating at 16 MHz and 1.17 T, and by pulsed FT (Fourier Transform) NMR, operating at 96.3 MHz and 7.05 T. A ^{11}B MAS-NMR spectrum was collected for one commercial sample (from Pfaltz and Bauer Chemical Company) at a spinning rate of 5 kHz using the pulsed spectrometer (a Bruker MSL-300 FT-NMR instrument). The parameters for the pulsed unit were as follows: a pulse length of 1–5 μs, a delay time of 10–20 μs and a repetition time of 1 s. For CW-NMR, a Varian V-4200B wide-line spectrometer was used along with a Nicolet 1170 signal averager. All of the ^{11}B NMR spectra were recorded at room temperature with a reference liquid of trimethyl borate ($(CH_3O)_3B$) employed for measurement of chemical shifts.

Since the NQR experiments require a large volume of sample ($\sim$30 ml), the NQR method was employed only for the five commercial $B_{12}C_3$ powders. All of the NQR responses were detected at 77 K using a Robinson-type [18] CW-NQR spectrometer [19].

10. Results

The ^{11}B NMR spectra for α-rhombohedral and β-boron obtained at 7.05 T revealed two peaks separated by 130–280 ppm (see figures 5 and 6). The two peaks for the coarse β-boron powder (figure 6(a)) were found at 114.4 and -150.2 ppm with respect to the ^{11}B reference frequency for trimethyl borate, while those for the fine β-boron powder (figure 6(b)) appear at 66.8 and -109.3 ppm. In addition, the ^{11}B NMR derivative spectra obtained at 1.17 T for α-rhombohedral boron and the fine β-boron powder revealed asymmetric peaks, and their integrated spectra showed a single broad peak (see figure 7). Figure 8(a) displays the ^{11}B NMR spectrum for the high-purity $B_{12}C_3$ powder at 7.05 Tesla: two peaks were centred at -96.9 and 47.8 ppm. The same lineshape was observed for a commercial $B_{12}C_3$ powder (from Pfaltz and Bauer) at 7.05 T (figure 8(b)). Figure 9 illustrates the ^{11}B CW-NMR spectra (1.17 T) for the high-purity $B_{12}C_3$ powder: an asymmetric central peak is seen together with two smaller peaks, appearing at about -9800 and 5400 ppm. A MAS-NMR spectrum (figure 10) for the commercial $B_{12}C_3$ powder revealed a single peak near (29 ppm along with spinning sidebands. Figure 11 displays the ^{11}B static NMR spectrum obtained at 7.05 T for ^{10}B enriched $B_{12}C_3$ powder: a dominant peak, near -23.1 ppm, is seen along with two smaller peaks, appearing at 311.9 and -314.3 ppm. The line width of the intense peak, appearing at -23.1 ppm, is reduced as compared with that of the central line (which is partially resolved into two lines) for the unenriched sample (figures 8(a) and 8(b)). The NMR data for this work are summarized in table 3.

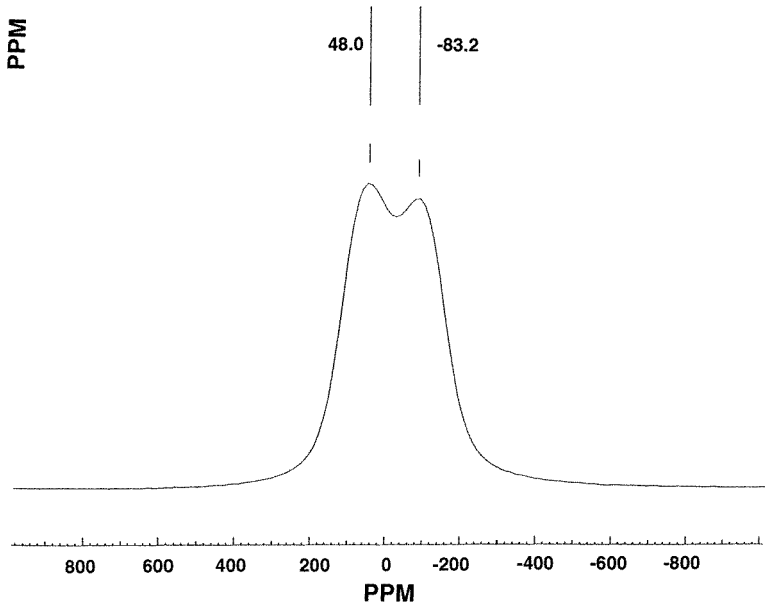

Figure 5. ^{11}B NMR spectrum for α-rhombohedral boron at 7.05 T obtained with the Bruker MSL-300 spectrometer. The two peaks are well separated.

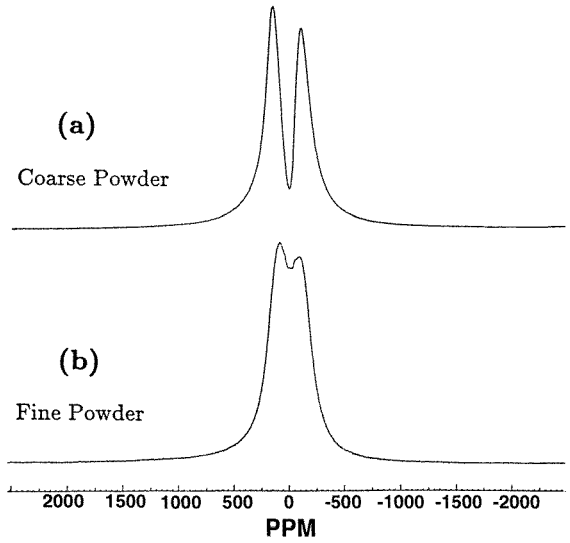

Figure 6. ^{11}B NMR spectra for the coarse (a) and fine (b) β-rhombohedral boron powders obtained at 7.05 T using the Bruker MSL-300 spectrometer. As for α-rhombohedral boron in figure 5, the two peaks are well resolved: two peaks for the coarse β-rhombohedral boron powder appear at 114.4 and -150.2 ppm, and those for fine β-rhombohedral boron powder appear at 66.8 and -109.3 ppm.

The boron NQR spectrum (figure 12) for the commercial $B_{12}C_3$ powder (from Pfaltz and Bauer) revealed a strong ^{11}B response at 2768.9 kHz and several other responses at lower

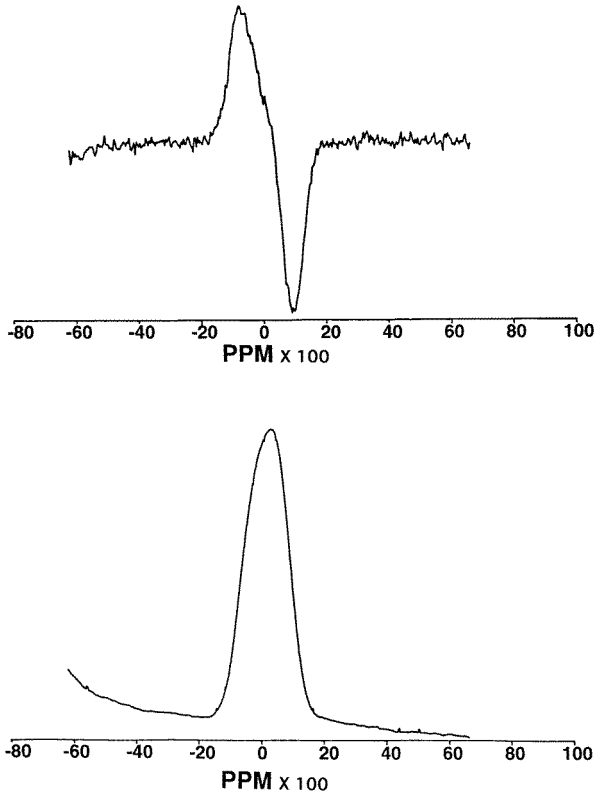

Figure 7. ^{11}B NMR responses in both derivative (top) and integrated (bottom) lines for α-rhombohedral boron at 1.17 T using the slow passage technique. The derivative line is clearly asymmetric whereas the integrated line, produced by integrating the derivative line on the signal averager, does not show the asymmetry as clearly. (This is generally the case with NMR spectra; asymmetry is more evident in the derivative.) The lineshapes for the fine β-rhombohedral boron powder are the same as these for α-rhombohedral boron.

Table 3. NMR data obtained from ^{11}B NMR spectra for icosahedral boron-rich solids: the peak positions were measured in ppm (parts per million). α-B is α-rhombohedral boron. β-B (a) and (b) are the coarse and fine β-rhombohedral boron powders, respectively.

Sample	Peak locations (ppm) at 7.05 T	Peak separation (kHz) at 7.05 T	$\Delta\nu_{FWHM}$ (kHz) at 1.17 T
α-B	48.0, −83.2	12.6	26.2
β-B (a)	114.4, −150.2	25.4	not tried
β-B (b)	66.8, −109.3	17.0	15.2
$B_{12}C_3$[a]	47.8, −96.9	13.9	17.8
$^{10}B_{12}C_3$[b]	−23.1	10.6 ($\Delta\nu_{FWHM}$)[c]	8.6

[a] High-purity unenriched $B_{12}C_3$.
[b] ^{10}B enriched boron carbide (enrichment of 90.61 at.%).
[c] Since only a single intense peak was obtained, the FWHM (full width at half maximum) was measured instead of a peak separation.

frequencies. All five commercial $B_{12}C_3$ powders had the same strong ^{11}B response within 6 kHz of that of the Pfaltz and Bauer sample. Other noticeable boron NQR responses, shown

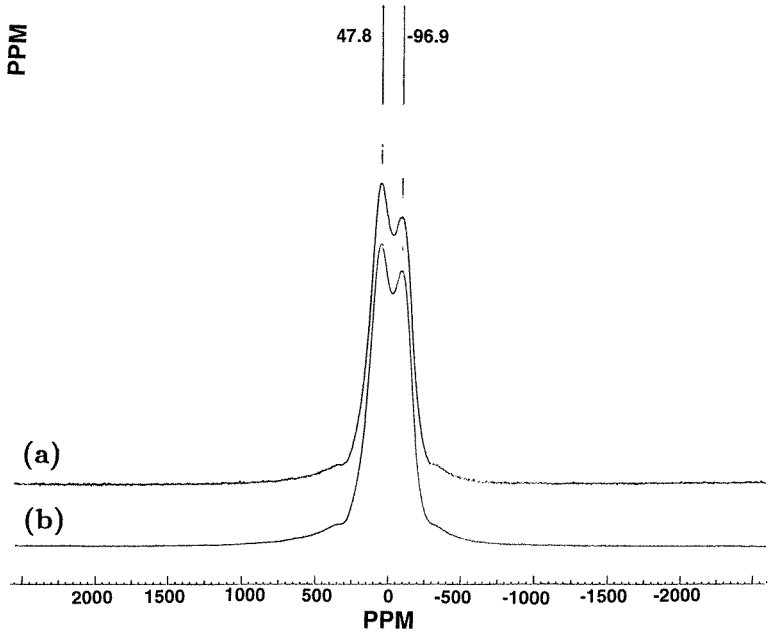

Figure 8. ^{11}B NMR spectra for unenriched highly purified (a) and unenriched commercial (b) boron carbide ($B_{12}C_3$) were obtained at 7.05 T using the Bruker MSL-300 spectrometer. The two spectra have the same lineshape and reveal at least three possible boron sites.

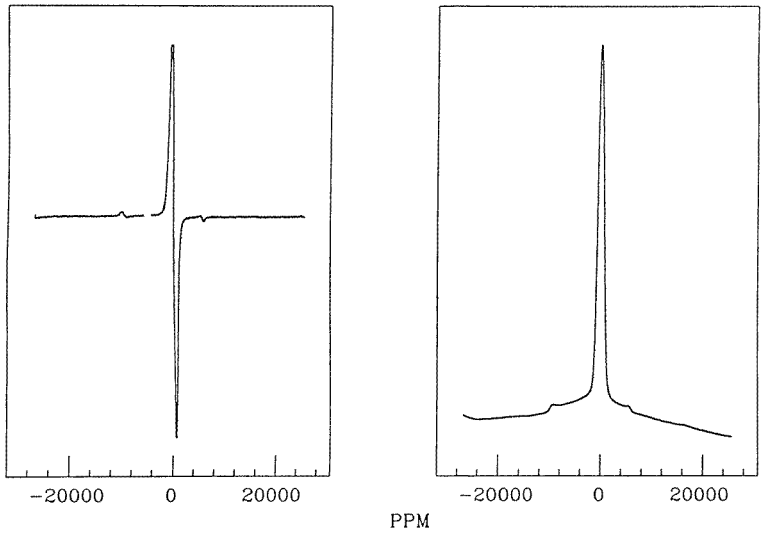

Figure 9. ^{11}B NMR responses for the unenriched highly purified $B_{12}C_3$ at 1.17 T obtained by the slow passage technique. A derivative line (left) is shown together with its integrated spectrum (right). The central line, which is clearly asymmetric in the derivative spectrum, is accompanied by smaller response on both sides of the central line.

in figure 12, were found at 361, 380 and 513 kHz. Because of the resemblance between the ^{11}B NMR spectra at 7.05 T for the high-purity $B_{12}C_3$ powder and the unenriched commercial $B_{12}C_3$ powder from Pfaltz and Bauer as shown in figures 8(a) and 8(b), only the spectra for

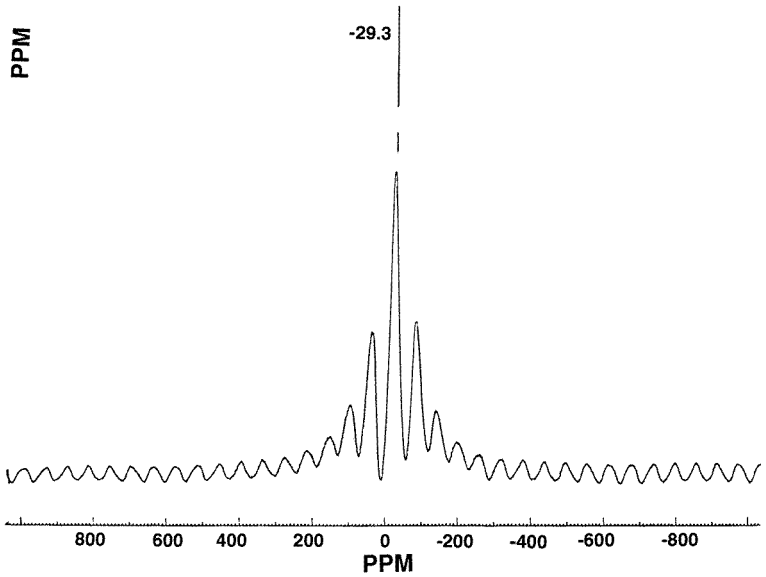

Figure 10. ^{11}B MAS-NMR spectrum for unenriched commercial $B_{12}C_3$ (from Pfaltz and Bauer) with a spinning rate of 5 kHz at 7.05 T. All the peaks except the strongest one are the spinning side bands.

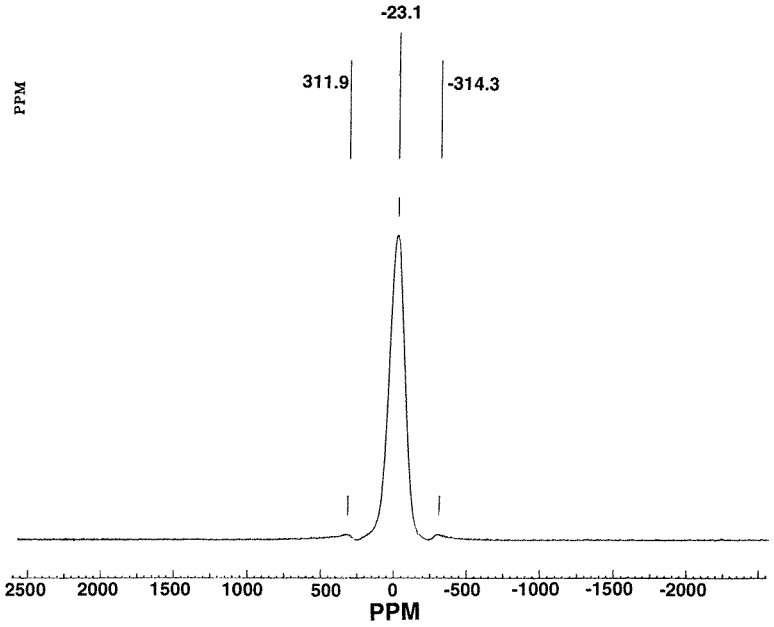

Figure 11. ^{11}B NMR spectrum for ^{10}B enriched (enrichment of 90.6 at.%) $B_{12}C_3$.

the Pfaltz and Bauer sample are displayed and discussed in this paper. The materials from the other commercial suppliers may possibly contain significant amounts of impurities (e.g. amorphous carbon) or be non-stoichiometric.

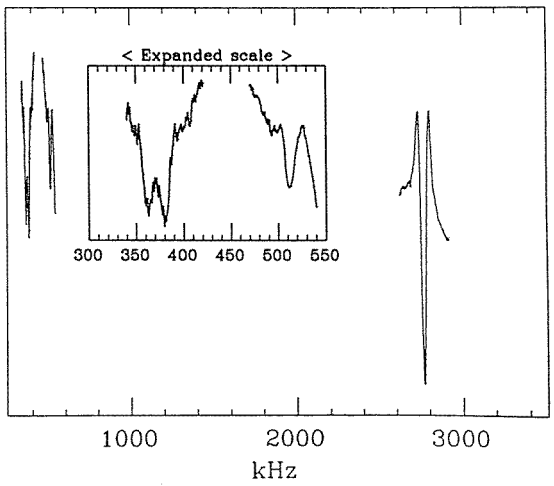

Figure 12. The complete set of boron NQR responses obtained for the unenriched commercial boron carbide from Pfaltz and Bauer. The inset with an expanded frequency scale is included to show the details of the resonances in the 300 to 550 kHz range.

11. Discussion

In addition to displaying two peaks at 7.05 T (figures 5, 6(a) and 6(b)) for α-rhombohedral boron and the coarse and fine β-boron powders, derivative ^{11}B NMR lines at 1.17 T (figure 7) are asymmetric suggesting the possibility of two distinct boron sites. The two sites are tentatively identified as the equatorial and the rhombohedral sites in the icosahedra. Since the two well resolved peaks at 7.05 T became a single broad absorption line at the lower field, 1.17 T, it is probable that the separation is due to the chemical shift interaction which decreases for weaker applied fields. Such significant chemical shifts have not been reported previously for ^{11}B NMR in boron-rich solids. For the two β-boron powders, the shift between the two peaks is decreased for the fine powder. This result raises the possibility that mechanical shock, experienced during the crushing process, may change the electron distribution at one or both sites. It is possible that a change in structure takes place. But contamination of the sample by impurities during the crushing process must also be considered.

Two major peaks were detected in the NMR spectra of $B_{12}C_3$, figures 8(a) and 8(b). The similarity of these two peaks to those found in α- and β-rhombohedral boron, figures 5 and 6, suggests a similar origin: chemical shift differences between boron atoms within equatorial, h_1, and rhombohedral, h_2, sites. This correlation suggests that the presence of carbon atoms within icosahedra does not noticeably perturb the EFG at the boron nuclei. In other words, differences between the ^{11}B NMR resonances of boron atoms in h_i and h_i^* sites are not measurable. Consistent with this notion, the internal bonding orbitals of icosahedral units are delocalized. Indeed, the bonding electrons may be simply described as being confined to the surface of the sphere circumscribing the atoms of the icosahedron [20]. We presume that measured differences in chemical shifts of icosahedral boron atoms relate to the bonds that they form to atoms outside the icosahedron.

The response at 47.8 ppm in figure 8 may be a superposition of responses due to h_1 and h_1^* sites (h_1 has been reported to have a Q_{cc} of less than 700 kHz [2, 3]); the peak at -96.9 ppm could be a superposition of responses from h_2 and h_2^* sites (h_2 has been reported to have a larger value of Q_{cc}, about 1 MHz [2, 3]). The Q_{cc} values of $\sim$700 kHz and $\sim$1 MHz are too

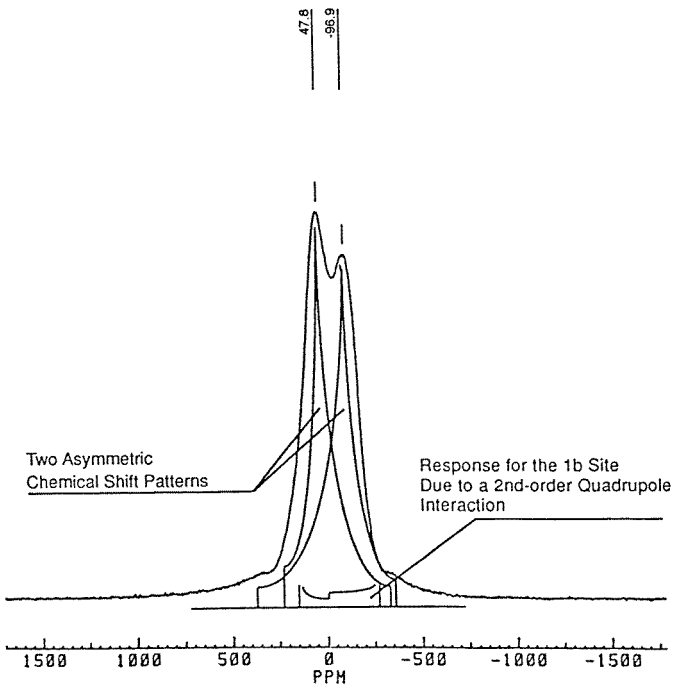

Figure 13. The separate responses of the high-field (7.05 T) NMR spectrum for unenriched $B_{12}C_3$.

small to yield observable second-order quadrupolar splittings [2] in the peaks observed for the polycrystalline powder at 7.05 T. However, the broadening [2] of the observed peaks by these quadrupolar effects will be larger for the larger value of Q_{cc} with a consequent reduction in the peak height. (The areas under the two peaks should be equal since the populations of the h_1, h_1^*, and h_2, h_2^* combinations are equal.) Since the peak at -96.9 ppm has the smaller height, it is assigned to the h_2, h_2^* combination.

In addition to the two intense peaks (figures 8(a) and 8(b)), another broad response is seen with its shoulders at about -340 and 370 ppm. These two shoulders could be formed in one of two possible ways: by the second-order quadrupolar interaction expected for ^{11}B in the 1b site, or by two different asymmetric (i.e. anisotropic) chemical shifts for ^{11}B in the icosahedral h_1 and h_2 sites. Figure 13 displays the two possibilities. In the latter case, the two observed intense peaks (figure 8) would arise from the divergences in the theoretical powder patterns for the two asymmetric chemical shifts, while the two small responses at about -340 and 370 ppm would be formed by the shoulders of the two powder patterns. (No broadening mechanisms have been added to the theoretical patterns in figure 13.) The second possibility is that the two small responses arise from the divergences in the theoretical lineshape for the expected second-order quadrupole interaction for ^{11}B in the 1b site. That theoretical lineshape (for the case $\eta = 0$) is shown in more detail by the dashed lines in figure 14 which also displays the actual lineshape (solid line) to be expected when the effects of broadening mechanisms are included (e.g. dipolar broadening, and distributions in the components of the electric field gradient (EFG) tensor caused by defects in the local composition or crystal structure). (The condition $\eta = 0$ applies to ^{11}B in the 1b site because of the threefold symmetry around the rhombohedral [111] direction (or the c axis of the hexagonal representation) [2].)

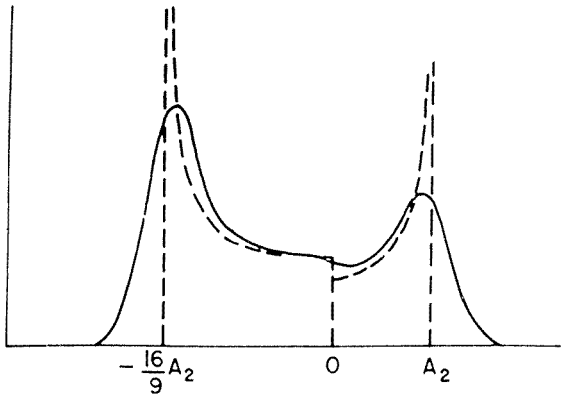

Figure 14. Theoretical lineshape (dashed lines) for the NMR response from a nucleus experiencing a large second-order quadrupole interaction. The solid line includes the effects of broadening mechanisms (e.g. dipolar broadening, distributions in the values of the components of the electric field gradient (EFG) tensor). For ^{11}B with spin $I = \frac{3}{2}$, the value of A_2 is $A_2 = \frac{3}{64}\ Q_{cc}^2/\nu_0$ where ν_0 is the Larmor resonance frequency in the absence of chemical shifts, quadrupole interactions, etc. Only the central, or $m = -\frac{1}{2} \leftrightarrow m = +\frac{1}{2}$ transition—which is the dominant or only transition usually detected—is shown.

^{11}B in the 1b site can be eliminated as a source of the small peaks at -340 and 370 ppm in figure 8. If one assumes that the two small peaks appearing at -9800 and 5400 ppm (at 1.17 T) in figure 9 locate the divergences in a second-order quadrupole pattern (figure 14), analysis (assuming $\eta = 0$) yields a value of $Q_{cc} = 5.5$ MHz which is in good agreement with the known value [2] for ^{11}B in the 1b site. The separation of the two small peaks (figure 9) for the 1b site will decrease at a higher field since the second-order quadrupole splitting varies as the inverse of the magnetic field. At 7.05 T (the field used to obtain the spectra in figure 8), they would appear at about -270 and 150 ppm, so they are lost underneath and within the observed spectrum (figure 8). The small peaks in the spectra displayed in figure 8 arise, then, from the two asymmetric chemical shifts. However, the two chemical shift interactions have a common feature. The MAS-NMR procedure used in obtaining the spectrum (figure 10) for the commercial $B_{12}C_3$ from Pfaltz and Bauer eliminates or reduces the effects of chemical shift asymmetry (and reduces the effect of second-order quadrupole interactions) on the NMR response. Only one peak (other than spinning sidebands) is observed, whose location is determined by the isotropic chemical shift asymmetry (when the quadrupole interaction) is small or zero. It would appear, then, that the sites giving rise to the two intense peaks in the static spectrum (figure 8) have approximately or exactly the same isotropic chemical shifts.

Unexpected results were obtained from the ^{11}B NMR study of the ^{10}B enriched $B_{12}C_3$ sample. It was expected that substitution of one boron isotope for another would leave the structural environment and hence the EFG for boron sites unaltered; however, the ^{11}B NMR spectrum (figure 11) for the ^{10}B enriched sample was vastly different from that of the unenriched sample. It consisted of one peak at -23.1 ppm, corresponding to the average of the two peaks in the unenriched sample, and two very small peaks to each side of it. The reduced line width of the dominant peak at -23.1 ppm is consistent with the expected [21] decrease in dipolar broadening caused by the fact that the magnetic dipole moment of ^{10}B differs from and is smaller than that of ^{11}B (i.e., the width of this *single* line is less than the width of either of the two partially resolved lines in the unenriched sample; see figure 8). It should be noted that for α-rhombohedral boron and β-boron, Tsiskarishvili *et al* [22] discovered that

the separation between the two peaks for the samples with the highest ^{11}B content decreased as the ^{10}B enrichment increased. They also suggested that the two peaks in the ^{11}B spectra could be produced by a second-order quadrupole interaction (see figures 8(a), 8(b) and 14) for a boron in one site (rather than being independent peaks from borons in two dissimilar sites). Also, they stated that the same effect does not occur in $B_{12}C_3$; but the present work shows that it does occur for the $B_{12}C_3$ used in the work reported here. Clearly, their suggestion that the two peaks observed for $B_{12}C_3$ and α-rhombohedral and β-boron at high magnetic fields could be caused by a second-order quadrupole interaction can be ruled out because the ^{11}B NMR spectrum at low field (1.17 T) shows only one peak (as expected for chemical shift effects) rather than the two more widely separated peaks (which would arise from a second-order quadrupole interaction). A satisfactory explanation for the collapse of the two peaks (observed at high magnetic fields) into one peak as the ^{10}B content is increased has not yet been devised. However, it should be noted that each of the samples was of different origin and form (solid mass, or powders of different particle size). For the best comparison, samples identical except for composition should be used, but these are not available.

The NQR response at 2768.9 ± 0.1 kHz (figure 12) corresponds to boron atoms in the 1b position. Using this NQR response and $\eta = 0$, the Q_{cc} value is calculated to be 5537.8 ± 0.2 kHz. Note that this Q_{cc} value is very close to the Q_{cc} values from NMR studies [2, 3]. The NQR measurement on a polycrystalline sample clearly yields much more accuracy for Q_{cc} than was obtained from NMR measurements on a single crystal [2], but the latter work—though requiring painstaking and very time-consuming measurements at many different orientations of the single crystal—did clearly establish the site giving rise to the response as the 1b site in a (CBC) chain rather than the (CCC) chain supported by Duncan [23].

Two more responses (figure 12), obtained at 361 and 380 kHz, could be either ^{11}B responses for the other boron sites in icosahedra or ^{10}B responses for the 1b site. (The ^{10}B nuclear isotope (spin $I = 3$) can yield as many as 13 NQR transitions [24] from which extremely accurate values of Q_{cc} and η can be obtained [25].) These NQR responses at frequencies less than 500 kHz were not consistent for each of the five commercial boron carbides. It is possible that the five boron carbide samples may contain somewhat different phases since the boron carbides ($B_{1-x}C_x$) can exist as a single-phase material with carbon concentrations (x) only between 0.1 and about 0.19–0.195 [8]. As noted earlier, another possibility is the presence of such inclusions as amorphous carbon.

Another noticeable response, as shown in figure 12, at 513 kHz may be assigned to one of the two icosahedral sites (h_2 and h_2^* sites) for ^{11}B or to the superposition of the responses from those two sites. The Q_{cc} value range for this response is calculated to be $889 \text{ kHz} \leqslant Q_{cc} \leqslant 1026$ kHz. (The range of values arises from equation (1) since the value of the asymmetry parameter is not known and can be any value between 0 and 1.) Since the values of Q_{cc} reported from NMR studies [2, 3] for the h_1-type site is less than 700 kHz, that site (now designated as h_1 and h_1^* to account for carbon in the icosahedra) is ruled out in favour of the h_2 (now h_2 and h_2^*) site whose Q_{cc} value from NMR [2, 3] is about 1 MHz.

12. Summary

Two peaks, separated by noticeable chemical shifts (130–280 ppm) in ^{11}B NMR spectra at 7.05 T, were observed for all unenriched icosahedral borides in this study, while only one peak was found for the ^{10}B enriched boron carbide powder (90.6 at.% of enrichment). The replacement of ^{11}B atoms with ^{10}B atoms not only reduced the line width but also yielded only one peak at the average position of the chemical shifts for the unenriched samples. When β-boron was crushed into a fine powder, the separation between the peaks was reduced,

which may reflect a change in the electron distribution at one or both boron sites that give rise to the two peaks, or the effect of impurities added during the crushing. A change in electron distribution could arise from a structural change in the material. The two types of site, present in each ^{10}B unenriched icosahedral boron-rich solid, may well be the equatorial and rhombohedral sites in the icosahedron which is the basic building block of each of the compounds. For $B_{12}C_3$, even though the icosahedral structure is altered by the presence of a carbon atom in the icosahedron, the two possible 'sites' (h_i and h_i^* with $i = 1$ or 2) for each location (equatorial and rhombohedral) may be very similar. In that case, the two ^{11}B NMR responses expected at high field (7.05 T) from each location would not be resolved (because of an insufficient difference in the chemical shifts), and only two peaks would appear in the NMR spectrum: one from borons in the h_1, h_1^* sites, the other from borons in the h_2, h_2^* sites.

Acknowledgments

The authors wish to emphasize that the appearance of two partially resolved peaks in the high-field ^{11}B NMR spectra for α-rhombohedral boron and β-boron, and the collapse of these peaks into a single line in samples highly enriched in the ^{10}B isotope, were discovered by Dr Gia Tsiskarishvili and his colleagues (see [22]). They are also much indebted to Dr Tsiskarishvili for providing the sample of α-rhombohedral boron used in the work reported here.

References

[1] Emin D 1987 *Mater. Res. Soc. Symp. Proc.* vol 97 (Pittsburgh. PA: Materials Research Society) p 3
[2] Silver A H and Bray P J 1959 *J. Chem. Phys.* **31** 247
[3] Hynes T V and Alexander M N 1971 *J. Chem. Phys.* **54** 5296
Hynes T V and Alexander M N 1972 *J. Chem. Phys.* Erratum **56** 681
[4] Decker B F and Kasper J S 1959 *Acta Crystallogr.* **12** 503
[5] Hughes R E, Kennard C H L, Sullenger D B, Weakliem H A, Sands D E and Hoard J L 1963 *J. Am. Chem. Soc.* **85** 361
[6] Zhdanov G S and Sevast'yanov N G 1941 *C.R. Acad. Sci. USSR* **32** 432
[7] Tallant D R, Aselage T L, Campbell A N and Emin D 1989 *Phys. Rev.* B **40** 5649
[8] Emin D, Samara G A, Azevedo L J, Venturini E L, Madden H H, Nelson G C, Shelnutt J A, Morosin N, Moss N and Wood C 1986 *J. Less-Common Met.* **117** 415
[9] Bouchacourt M and Thevenot F 1981 *J. Less-Common Metals* **82** 227
[10] Aselage T L and Tissot R G 1992 *J. Am. Ceram. Soc.* **75** 2207
[11] Clark H K and Hoard J L 1943 *J. Am. Chem. Soc.* **65** 2115
[12] Aselage T L and Emin D 1991 *AIP Conf. Proc.* vol 231 (Woodbury, NY: AIP) pp 177–85
[13] Aselage T L, Tallant D R and Emin D 1997 *Phys. Rev.* B **56** 3122
[14] Alelage T L and Talant D R 1998 *Phys. Rev.* B **57** 2675
[15] Morosin D, Mullendore A W, Emin D and Slack G A 1985 *AIP Conf. Proc.* vol 140 (Woodbury, NY: AIP) pp 70–86
[16] Bersohn R 1952 *J. Chem. Phys.* **20** 1505
[17] Aselage T L and Tissot R G 1992 *J. Am. Ceram. Soc.* **75** 2207
[18] Robinson F N H 1982 *J. Phys. E: Sci. Instrum.* **15** 814
[19] Gravina S 1989 *PhD Thesis* Brown University
[20] Emin D, Evans D G and McCready S S 1998 *Phys. Status Solidi* b **205** 31
[21] Abragam A 1961 *The Principles of Nuclear Magnetism* (Oxford: Oxford University Press)
[22] Tsiskarishvili G A, Lundström T, Tegenfelt J, Doldze T V and Tsagareishvili G V 1990 *Proc. 10th Int. Symp. on Boron, Borides, and Related Compounds (Albuquerque, NM, 1990); AIP Conf. Proc.* vol 231 (Woodbury, NY: AIP) pp 280–8
[23] Duncan T M 1983 *J. Am. Chem. Soc.* **106** 2270
[24] Creel R B 1982 *J. Magn. Reson.* **50** 82
[25] Gravina S J, Bray P J and Petersen G L 1990 *J. Non-Cryst. Solids* **123** 165